



# Comparison of two Gaia sphere solutions using orthonormal bases on the sphere

prepared by: B. Bucciarelli, U. Abbas, A. Vecchiato, M. G. Lattanzi
approved by: Mario G. Lattanzi
reference: GAIA-C3-TN-INAF-BB-002-01
issue: 01
revision: 0
date: 15-05-2011
status: Issued

# Abstract

This note describes the application of an analytical model for the comparison of angular positions, proper motions and parallaxes generated by two Gaia sphere solutions.

# Contents

# 1 Introduction

The use of Vector Spherical Harmonics for catalog-to-catalog comparison is known in the astronomical literature (see Arias et al. (2000); Mignard & Morando (1990); Walter & Sovers (2000)). In this technical note we review the theoretical foundations of the method and illustrate how it is applied in practice. We show that this approach can be powerful in estimating global and local systematic differences possibly present between two Gaia sphere solutions. Some results on simulated data are presented.

## 1.1 Objectives

This technical note explains the steps implemented to perform the task described in the above section, and shows the results of some tests conducted with the Fortran implementation of such procedure. These results will be used for the initial verification of the Java implementation, which will be the subject of another forthcoming note.

## 1.2 References

Arias, E.F., Cionco, R.G., Orellana, R.B., Vucetich, H., 2000, A&A, 359, 1195, ADS Link

**[BB-001]**, Bucciarelli, B., Abbas, U., Vecchiato, A., et al., 2011, *Link between two Gaia intermediate sphere solutions*,
GAIA-C3-TN-INAF-BB-001,
URL http://www.rssd.esa.int/llink/livelink/open/3060355

Mignard, F., Morando, B., 1990, In: N. Capitaine & S. Débarbat (ed.) Journées 1990: Systèmes de Référence Spatio-Temporels, 151–158, ADS Link

Schwan, H., 2001, A&A, 367, 1078, ADS Link

Walter, H.G., Sovers, O.J., 2000, *Astrometry of Fundamental Catalogues*, Springer, 1 edn.

## 1.3 Acronyms

The following is a complete list of acronyms used in this document. The following table has been generated from the on-line Gaia acronym list:

| Acronym | Description |
|---|---|
| VSH | Vector Spherical Hermonics |

# 2 Vector Spherical Harmonics: theoretical background and notations

If we assume that the angular differences $\Delta\alpha\cos\delta$, $\Delta\delta$ between two catalogs constitute a vector field $\mathbf{V}_{pos}(\alpha,\delta)$ on the unit sphere, then we can represent such a field with a series expansion using some particular vector functions, viz.:

$$\mathbf{V}_{\rm pos}(\alpha,\delta) = \sum_{l}\sum_{m=-l}^{l}\left(s_{lm}\mathbf{\Psi}_{lm}(\alpha,\delta) + t_{lm}\mathbf{\Phi}_{lm}(\alpha,\delta)\right) \tag{1}$$

The functions $\mathbf{\Phi}_{lm}$ and $\mathbf{\Psi}_{lm}$ are, respectively, the spheroidal (or electric) and toroidal (or magnetic) Vector Spherical Harmonics (VSH) of order $(l,m)$, which are defined as (Barrera et al. 1985 and references therein):

$$\mathbf{\Phi}_{lm} \equiv \frac{\nabla Y_{lm}}{\sqrt{l(l+1)}} = \frac{1}{\sqrt{l(l+1)}}\left(\frac{\partial Y_{lm}}{\partial\delta}\mathbf{e}_\delta + \frac{1}{cos\delta}\frac{\partial Y_{lm}}{\partial\alpha}\mathbf{e}_\alpha\right) \tag{2}$$

$$\mathbf{\Psi}_{lm} \equiv \frac{\mathbf{e}_r\times\nabla Y_{lm}}{\sqrt{l(l+1)}} = \frac{1}{\sqrt{l(l+1)}}\left(\frac{\partial Y_{lm}}{\partial\delta}\mathbf{e}_\alpha - \frac{1}{cos\delta}\frac{\partial Y_{lm}}{\partial\alpha}\mathbf{e}_\delta\right) \tag{3}$$

where $(\mathbf{e}_\alpha,\mathbf{e}_\delta,\mathbf{e_r})$ are unit vectors forming a normal triad with origin in $(\alpha,\delta)$, (see Fig. 1), whose components in the cartesian frame associated with the equatorial reference system are given by

$$\mathbf{e}_\alpha = \begin{bmatrix} -\sin\alpha \\ \cos\alpha \\ 0 \end{bmatrix} \qquad \mathbf{e}_\delta = \begin{bmatrix} -\cos\alpha\ \sin\delta \\ -\sin\alpha\ \sin\delta \\ \cos\delta \end{bmatrix} \qquad \mathbf{e_r} = \begin{bmatrix} \cos\alpha\ \cos\delta \\ \sin\alpha\ \cos\delta \\ \sin\delta \end{bmatrix} \tag{4}$$

and

$$Y_{lm}(\alpha,\delta) = \sqrt{\frac{(2l+1)(l-m)!}{4\pi(l+m)!}}P_l^m(\sin\delta)\,e^{im\alpha} \tag{5}$$

are the canonical scalar spherical harmonics defined in terms of the associated Legendre polynomial $P_l^m(x)$.

The functions $\mathbf{\Phi}$ and $\mathbf{\Psi}$ form a set of basis functions on the sphere; they satisfy the orhonormal conditions over $4\pi$ radians, i.e.,

$$\int \mathbf{\Phi}_{lm}\mathbf{\Phi}^*_{l'm'}d\Omega = \delta_{ll'}\delta_{mm'}, \qquad \int \mathbf{\Psi}_{lm}\mathbf{\Psi}^*_{l'm'}d\Omega = \delta_{ll'}\delta_{mm'}, \qquad \mathbf{\Phi}_{lm}\cdot\mathbf{\Psi}_{lm} = 0$$

and, in analogy with scalar spherical harmonics, have the following property:

$$\mathbf{\Phi}_{l,-m} = (-1)^m\mathbf{\Phi}^*_{lm}, \qquad \mathbf{\Psi}_{l,-m} = (-1)^m\mathbf{\Psi}^*_{lm}$$

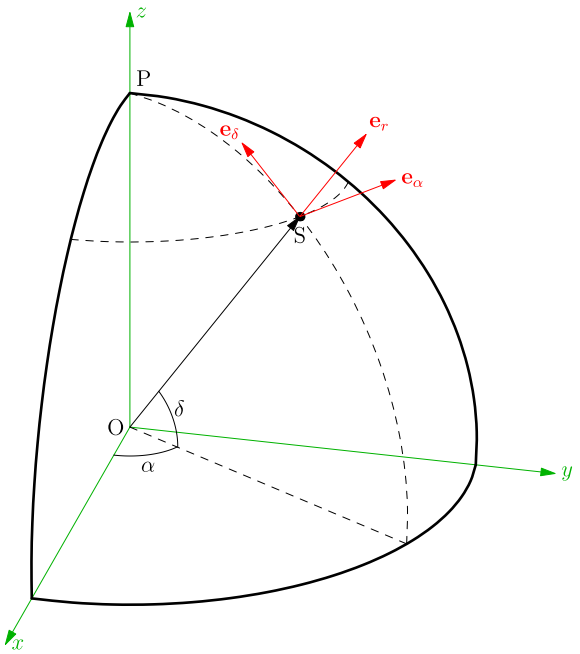


FIGURE 1: The normal triad $(\mathbf{e}_\alpha, \mathbf{e}_\delta, \mathbf{e}_\mathbf{r})$ associated with star S

where the asterisk symbol indicates the complex conjugate.

By enforcing the orthogonality conditions, the coefficients $t_{lm}$ and $s_{lm}$ can be computed from:

$$t_{lm} = \int \mathbf{\Psi}^*_{lm} \cdot \mathbf{V} d\Omega, \quad s_{lm} = \int \mathbf{\Phi}^*_{lm} \cdot \mathbf{V} d\Omega$$

As in the case of spherical harmonics, each VSH shows a characteristic periodicity over the sphere, with frequency depending on its order $(l, m)$; this property is visualized in Fig. 2 which displays four particular VSH functions of orders 1 and 2.

# 3 The Vector Fields of Angular Positions and Proper Motions

Taking into account the conjugation symmetry property, and the fact that we are dealing with real functions, the finite series expansion (1) is reduced to:

$$\begin{aligned}\mathbf{V}_{\rm pos}(\alpha,\delta) \;=\; V_\alpha \mathbf{e}_\alpha + V_\delta \mathbf{e}_\delta = & \sum_{l=1}^{l_{max}} [t^R_{l0}\mathbf{\Psi}^R_{l0} + s^R_{l0}\mathbf{\Phi}^R_{l0} \\ & +2\sum_{m=1}^{l_{max}} (t^R_{lm}\mathbf{\Psi}^R_{lm} - t^I_{lm}\mathbf{\Psi}^I_{lm} + s^R_{lm}\mathbf{\Phi}^R_{lm} - s^I_{lm}\mathbf{\Phi}^I_{lm})] \quad (6)\end{aligned}$$

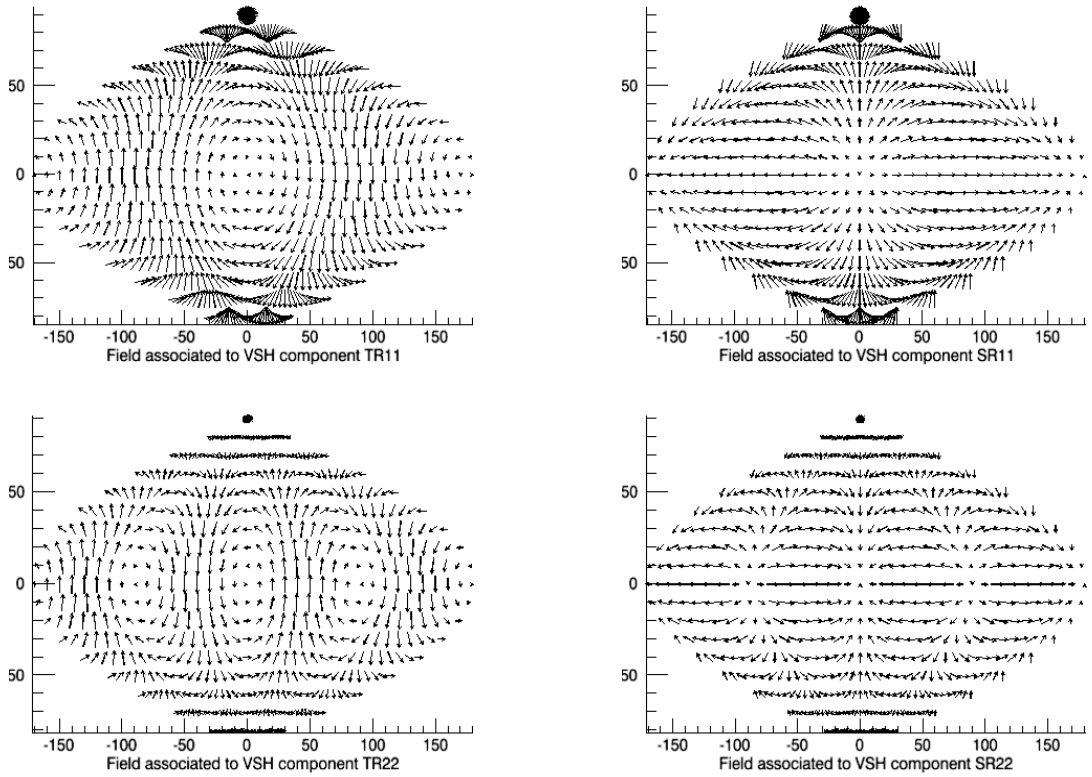


FIGURE 2: Visualization of the vector fields associated with the VSH functions $\mathbf{\Psi}_{11}^{R}$ (top left), $\mathbf{\Phi}_{11}^{R}$ (top right), $\mathbf{\Psi}_{22}^{R}$ (bottom left), and $\mathbf{\Phi}_{22}^{R}$ (bottom right)

where the superscripts *R, I* denote the real and imaginary part of the function. This representation applies as well to the vector field $\mathbf{V}_{\rm pm}(\alpha,\delta)$ of proper motion residuals $\Delta\mu_\alpha\cos\delta, \Delta\mu_\delta$.

The development in series of VSH, compared to the more classical scalar approach (see e.g. Schwan (2001)), has the advantage of treating the vectorial nature of the angular position (or proper motion) differences, which results in a clear separation between global and local systematic effects, as illustrated in the following.

If the two catalogs differ for an *infinitesimal rotation* represented by a rotation vector $\boldsymbol{\omega}(\epsilon_x,\epsilon_y,\epsilon_z)$, with components given in the equatorial system, the associated vector field is given by:

$$\mathbf{V}(\alpha,\delta) = (-\epsilon_x\ \sin\alpha + \epsilon_y\ \cos\alpha)\mathbf{e}_\delta + (-\epsilon_x\ \cos\alpha\sin\delta - \epsilon_y\ \sin\alpha\sin\delta + \epsilon_z\ \cos\delta)\mathbf{e}_\alpha$$

Moreover, let us assume the presence of a global *glide* characterized by an irrotational vector $\mathbf{g}(g_x,g_y,g_z)$, with an associated vector field of the form:

$$\mathbf{V}(\alpha,\delta) = g_x\ \mathbf{e}_\alpha + g_y\ \mathbf{e}_\delta + g_z\ \mathbf{e}_r$$

It can be demonstrated that these two global effects are packed in the $l = 1$ coefficients, more

specifically:

$$\epsilon_x = -\sqrt{\frac{3}{4\pi}} t^R_{11}, \quad \epsilon_y = \sqrt{\frac{3}{4\pi}} t^I_{11}, \quad \epsilon_z = \sqrt{\frac{3}{8\pi}} t^R_{10} \tag{7}$$

and

$$g_x = -\sqrt{\frac{3}{4\pi}} s^R_{11}, \quad g_y = \sqrt{\frac{3}{4\pi}} s^I_{11}, \quad g_z = \sqrt{\frac{3}{8\pi}} s^R_{10} \tag{8}$$

The presence of these and other systematic effects can be detected by testing the significance of the different expansion coefficients.

# 4 The Scalar Field of Parallaxes

Parallax residuals can be seen as the radial part of a vector field costituted by the spatial positions differences on the celestial sphere; however, noticing that VSH have the property of separating the angular part from the radial one when using spherical coordinates, the parallax residuals can be treated independently from the angular positions and analysed using scalar spherical harmonics, as follows

$$V_\pi(\alpha, \delta) = \Delta\pi = \sum_l \sum_{m=-l}^{l} c_{lm} Y_{lm}(\alpha, \delta) \tag{9}$$

where $Y_{lm}$ has been defined in the previous sections, and $\pi$ is the star's parallax. Enforcing the reality condition, Eq. (9) reduces to:

$$\Delta\pi = \sum_{l=1}^{l_{max}} [c^R_{l0} Y^R_{l0} + 2 \sum_{m=1}^{l_{max}} (c^R_{lm} Y^R_{lm} - c^I_{lm} Y^I_{lm})] \tag{10}$$

where, as in Eq. (6), the superscripts *R, I* denote the real and imaginary part of $Y_{lm}$.

# 5 Least-Squares Adjustment

The coefficients of the VSH series expansion are estimated through a least-squares adjustment of a set of catalog-to-catalog differences. In the case of angular positions, each star provides two observation equations, namely, the right-ascension and declination components of the vector equation (6). In the case of parallax, Eq. (10) provides one observation equation per star. In both cases, catalog errors should be used to weight the respective observation equation. Assuming that the correlations between errors in the astrometric parameters of different objects can be neglected, the variance-covariance matrix of the RHS vector becomes diagonal (cfr. BB-001); therefore, we can obtain the weighted least-squares system by multiplying the equation relative

to object $i$ by the following normalized weight

$$p_\Delta(i) = \frac{\sigma_\Delta}{\sigma_\Delta(i)}, \quad \text{with} \quad \frac{1}{\sigma_\Delta^2} = \frac{1}{N}\sum_{i=1}^{N}\frac{1}{\sigma_\Delta^2(i)} \quad \text{and} \quad \sigma_\Delta^2 = \sigma_1^2 + \sigma_2^2 - 2\rho_{12}\sigma_1\sigma_2$$

Here $\sigma_\Delta$ stands for the standard deviation of the residual of the generic astrometric parameter, $N$ is the total number of objects, and the subscripts $(1, 2)$ are indices identifying the two catalogs. The number of parameters to be estimated is given by $2l_{\max}^2 + 4l_{\max}$ (or $l_{\max}^2 + 2l_{\max}$ for the parallax case), with $l_{\max}$ representing the maximum degree of the series expansion. This parameter is not a priori fixed, and in general can be adjusted by examining the RMS of the fit:

$$\mathrm{RMS} = \sqrt{\frac{\sum_{i=1}^{N}(V(i)_{\mathrm{obs}} - V(i)_{\mathrm{calc}})^2 \cdot p_\Delta(i)^2}{M - N}} \tag{11}$$

where $M$ and $N$ are the number of system rows and columns respectively. The RMS is also used to calculate the normalized chi-square test as $\chi^2 = (M - N) \times \mathrm{RMS}^2/\sigma_\Delta^2$, which is close to unity when the data is adequately represented by the adopted model.

# 6 A Test Example

To test the fortran code we have compared the positions of a simulated catalog of 10,000 stars (CATR) with those of a second catalog (CATC) to which we have applied a random perturbation with standard deviation of 50 $\mu$as plus a rotation $\boldsymbol{\omega}(\epsilon_x, \epsilon_y, \epsilon_z)$, with $\epsilon_x = \epsilon_y = \epsilon_z = 57.735$ $\mu$ as and a glide $\mathbf{g}(g_x, g_y, g_z)$, with $g_x = g_y = g_z = 100$ $\mu$as. The esimated coefficients of the VSH expansion used for the fit ($l_{\max} = 5$) were all negligible except from those corresponding to $l = 1$ which resulted of the order of $10^{-10}$ radians. The rotation and glide parameters estimated using formulas (7) and (8) are perfectly consistent with the simulated values at the micro-arcsecond level, as shown in Tab. 1. The graphs of Fig. 3 show the differences in right ascension and declination between CATR and CATC before and after subtraction of the estimated systematic differences.

| Parameter (see text) | True ($\mu$as) | Adjusted ($\mu$as) | $\sigma$ ($\mu$as) |
|---|---|---|---|
| $\epsilon_x$ | 57.735 | 57.89 | 0.60 |
| $\epsilon_y$ | 57.735 | 57.05 | 0.60 |
| $\epsilon_z$ | 57.735 | 57.87 | 0.60 |
| $g_x$ | 100.000 | 99.74 | 0.60 |
| $g_y$ | 100.000 | 100.00 | 0.60 |
| $g_z$ | 100.000 | 100.30 | 0.60 |

TABLE 1: Simulated and fitted values of the *rotation* and *glide* parameters retrieved by comparing two catalogues of 10,000 stars having random errors of 50 $\mu$as

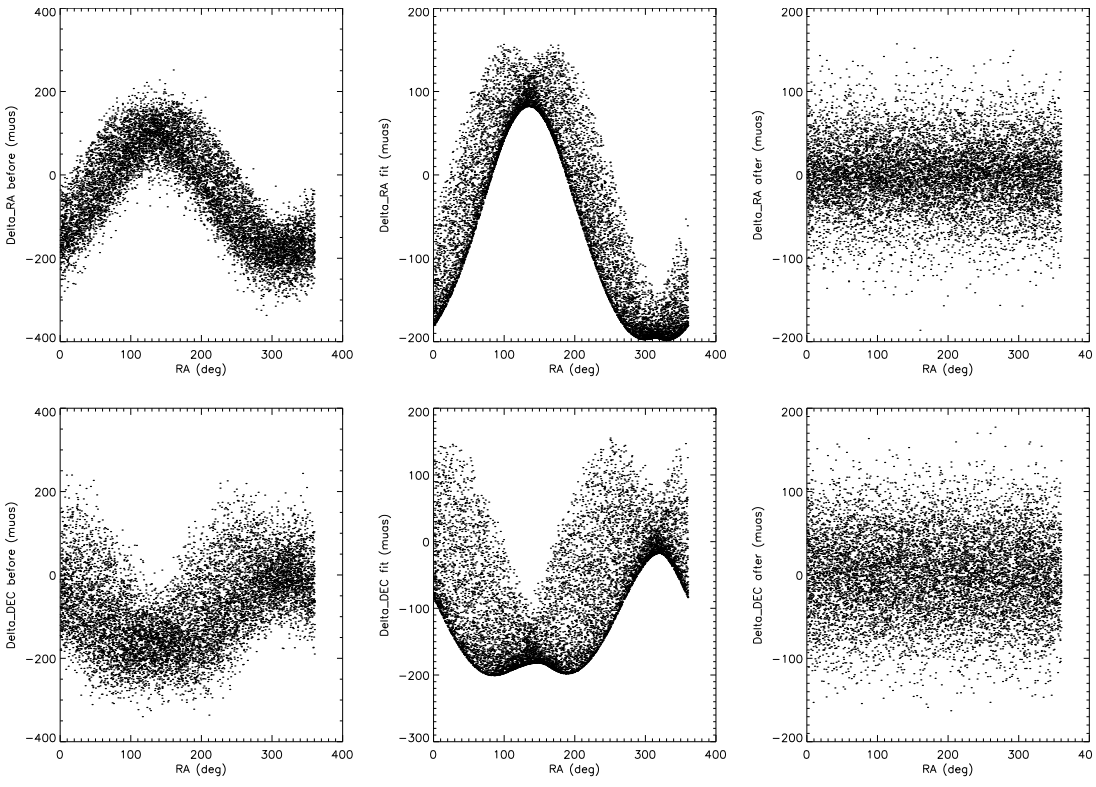


FIGURE 3: Analysis of the residuals in Right Ascension (top panels) and Declination (bottom panels) between two simulated catalogs. The graphs show the differences in R.A. and DEC before (left) and after (right) elimination of the fitted systematics, which are plotted in the central graphs.